

## Oral administration of paclitaxel with PEGylated poly(anhydride) nanoparticles: Permeability and pharmacokinetic study

Virginia Zabaleta<sup>1</sup>, Gilles Ponchel<sup>2,3</sup>, Hesham Salman<sup>1</sup>, Maite Agüeros<sup>1</sup>,  
Christine Vauthier<sup>2,3</sup>, Juan M. Irache<sup>1</sup>

<sup>1</sup> University of Navarra. Department Pharmacy and Pharmaceutical Technology.  
Pamplona, Spain

<sup>2</sup> Univ Paris-Sud, Physicochimie, Pharmacotechnie, Biopharmacie, UMR 8612,  
Chatenay-Malabry, F-92296.

<sup>3</sup> CNRS, Chatenay-Malabry, F-92296.

### Corresponding author:

Juan M. Irache  
Dep. Pharmacy and Pharmaceutical Technology  
University of Navarra  
31080 – Pamplona  
Spain  
Tel: +34948425600  
e-mail: [jmirache@unav.es](mailto:jmirache@unav.es)

## **Abstract**

The aim of this work was to study the potential of pegylated poly(anhydride) nanoparticles as carriers for the oral delivery of paclitaxel (PTX). Paclitaxel is an anticancer drug, ascribed to the class IV of the Biopharmaceutical Classification system, characterised for its low aqueous solubility and to act as a substrate of the P-glycoprotein and cytochrome P450.

For the pegylation of nanoparticles, three different poly(ethylene glycol) (PEG) were used: PEG 2000 (PTX-NP2), PEG 6000 (PTX-NP6) and PEG 10000 (PTX-NP10). The transport and permeability of paclitaxel through the jejunum mucosa of rats was determined in Ussing chambers whereas its oral bioavailability was studied in rats.

The loading of PTX in pegylated nanoparticles increased between 3 and 7-times the intestinal permeability of paclitaxel through the jejunum compared with the commercial formulation Taxol®. Interestingly, the permeability of PTX was significantly higher for PTX-NP2 and PTX-NP6 than for PTX-NP10.

In the in vivo studies similar results were obtained. When PTX-NP2 and PTX-NP6 were administered to rats by the oral route, sustained and therapeutic plasma levels of paclitaxel for at least 48-h were observed. The relative oral bioavailability of paclitaxel delivered in nanoparticles was calculated to be 70% for PTX-NP2, 40% for PTX-NP6 and 16% in case of PTX-NP10.

All of these observations would be related with both the bioadhesive properties of these carriers and the inhibitory effect of PEG on the activity of both P-gp and P450 cytochrome.

**Key words:** nanoparticles, paclitaxel, poly(ethylene glycol), bioadhesion, oral, drug delivery, controlled release.

## Introduction

Paclitaxel ( $C_{47}H_{51}NO_{14}$ ) is a pseudoalkaloid with a diterpenoid structure and a molecular weight of 853 Da [1]. Originally, it was extracted from the bark of the Pacific yew tree (*Taxus brevifolia*). Nowadays, it is obtained from the natural precursor product 10-deacetyl baccatin III (10-DAB), available in sufficient quantities from the European yew tree (*Taxus Baccata*), which is transformed into taxol by a semi-synthetic production process consisted in seven chemical steps [2].

Paclitaxel acts as an antineoplastic agent due to its inhibitory effect of cellular growth by stabilizing the microtubule assembly and, thus, blocking the cell replication in the late G2 mitotic phase of the cell cycle [3]. This anticancer drug is widely used in the treatment of several carcinomas including breast [4], advanced ovarian [5], non small cell lung [6] and colon [7]. In addition, paclitaxel is also employed for the treatment AIDS related Kaposi's sarcoma [8].

Paclitaxel is administered to patients via intravenous infusion. Since paclitaxel is practically water insoluble with a very low aqueous solubility of less than 0.3 mg/ml [9], the commercial formulations (i.e. Taxol®, Paxene®) include a mixture of Cremophor EL (polyoxyethylated castor oil) and ethanol (1:1, w/w) as solvent [10]. However, the use of Cremophor EL is associated with hypersensitivity reactions [11] and causes leakage of plasticizers from polyvinyl chloride (PVC) infusion bags and polyethylene tubing [12]. In addition, it has been demonstrated that this pharmaceutical excipient alters the pharmacokinetic behaviour of many drugs administered intravenously, including paclitaxel, by increasing the systemic exposure to the drug and reducing the systemic clearance [13].

In the last years, a number of efforts have been performed in order to develop paclitaxel oral formulations. This new approach would offer advantages over intravenous infusion such as more attractive for patients and would enable the development of chronic treatment schedules resulting in sustained plasma concentrations above a pharmacologically relevant threshold level [14]. Unfortunately, paclitaxel shows a limited bioavailability (<10%) when administered orally [15]. This effect is mainly due to its low aqueous solubility and dissolution as well as its affinity for intestinal cytochrome P-450 metabolic enzymes (i.e. CYP3A4) and the multidrug efflux transporter P-glycoprotein (P-gp) [16].

In order to overcome these problems and to enhance the oral bioavailability of this anticancer drug, a number of strategies have been proposed. Among others, the most popular has been the synthesis of oral absorbable paclitaxel analogs and its association or co-administration with a P-gp inhibitor. Thus, paclitaxel derivatives such as BMS-275183 [17] and ortataxel [18] have been proposed for oral delivery of this anticancer drug. For BMS-275183, its oral bioavailability in humans was found to be 24% [17]; although its clinical use is limited by its toxicity, mainly related with the induction of peripheral neuropathies [17]. For ortataxel, which is not recognised by P-glycoprotein, its oral bioavailability was found to be close to 50% [19]. However, its antitumoral efficacy is reduced and/or its use may be hampered by its haematological toxicity [20].

In parallel, another strategy for the improvement of the oral bioavailability of paclitaxel has been the design of pharmaceutical formulations able to solubilise the drug and, at the same time, to promote its mucosal permeability. In this

aspect, drug delivery systems such as micelles [21], niosomes [22], or PLGA nanoparticles have been proposed [23]. Another interesting alternative for the formulation of paclitaxel was the use of self-emulsifying or self-microemulsifying drug delivery systems [24, 25]. These formulations can contain components which act as Pgp/ cytochrome P-450 inhibitors such as polysorbate 20, polysorbate 80, Solutol® surfactants and vitamin E TPGS [26]. Pharmacokinetic studies conducted in rats showed that the oral bioavailability of paclitaxel in a supersaturable self-emulsifying drug delivery systems was about 5-times higher than the control [24]. In a similar way, more recently, new solid lipid nanocapsules (containing Solutol® HS15) have demonstrated a high ability to promote the oral absorption of paclitaxel in rats [15].

In this context, another approach may be the use of pegylated poly(anhydride) nanoparticles. These carriers have been demonstrated a high ability to develop bioadhesive interactions within the gut [27] and would facilitate the localisation of paclitaxel in close contact with the surface of absorptive cells of the intestine. In addition, the presence of poly(ethylene glycol) (PEG) can add a supplementary advantage. In fact, it has been described that PEG can negatively affect the activity of the P-gp [28] and the CYP isoenzyme 3A4 [29]. Thus, the aim of this work was to study the potential of pegylated poly(anhydride) nanoparticles as carriers for the oral delivery of paclitaxel. For this purpose, pegylated nanoparticles containing paclitaxel were optimized and the intestinal permeability of paclitaxel was investigated using the Ussing chamber method. Finally, the pharmacokinetics of paclitaxel when incorporated in these bioadhesive carriers was also evaluated in rats.

## **2. Materials and methods**

### **2.1. Chemicals**

Poly(methyl vinyl ether-co-maleic anhydride) or PVM/MA (Gantrez® AN 119; MW 200,000) was kindly gifted by ISP (Barcelona, Spain). Verapamil, glycine and glutamine were provided by Sigma–Aldrich (Steinheim, Germany). 2-hydroxypropyl-β-cyclodextrin (HPCD) by RBI (Massachusetts, USA). Poly(ethylene glycol) with Mw of 2000, 6000 and 10000 Da (PEG 2000; PEG 6000; PEG 10000) and disodium edetate (EDTA) were supplied by Fluka (Switzerland). Paclitaxel (USP 26 grade >99.5%) was purchased by 21CEC (London, United Kingdom). Docetaxel (Taxotere®) was provided by Sanofi-Aventis (Paris, France). Taxol® was purchased from Bristol-Myers Squibb (New York, USA). Acetone and ethanol were obtained from VWR Prolabo (Fantenay sous Bois, France). Rhodamine B isothiocyanate (RBITC) were supplied by Sigma (St Louis, USA). Bumetanide was provided by Calbiochem (Meudon, France). Deionised reagent water (18.2 MΩ resistivity) was prepared by a water purification system (Wasserlab, Pamplona, Spain). All other chemicals used were of analytical grade and obtained from Merck (Darmstadt, Germany).

### **2.2. Preparation of pegylated poly(anhydride) nanoparticles**

Paclitaxel (PTX) was encapsulated in either conventional or pegylated poly(anhydride) nanoparticles by a modification of the solvent displacement procedure previously described for the preparation of these functionalized nanoparticles [27]. Three different types of poly(ethylene glycols) were used: PEG 2000, PEG 6000 and PEG 10000.

#### **2.2.1. Paclitaxel-loaded pegylated poly(anhydride) nanoparticles**

Poly(ethylene glycol) (12.5 mg) was firstly dispersed in 3 ml of acetone and added to a solution of 100 mg of the copolymer of methyl vinyl ether and maleic anhydride (Gantrez® AN 119) in 2 ml of the same organic solvent. The resulting mixture was maintained under magnetic agitation. On the other hand, paclitaxel was dissolved in 0.5 ml of acetone and added to the polymers mixture. Then, the organic phase containing PTX, PVM/MA and PEG was magnetically stirred for 1 h at room temperature. After this time, nanoparticles were formed by the addition of 10 ml of ethanol followed by the addition of 10 ml of an aqueous solution containing glycine (50 mg) and disodium edetate (20 mg). After homogenisation for 10 min, the organic solvents were eliminated by evaporation under reduced pressure (Büchi R-144, Switzerland) and the resulting suspensions purified by tangential filtration in Vivaspin tubes at 3000xg for 20 min. The supernatants were removed and the pellets resuspended in water. The purification process was repeated twice and finally, the formulations were frozen and then freeze-dried (Genesis 12EL, Virtis, USA) using sucrose (5%) as cryoprotector.

For the identification of the different formulations the following abbreviations were used: PTX-NP2 (with PEG 2000), PTX-NP6 (with PEG 6000) and PTX-NP10 (with PEG 10000).

### **2.2.2. Paclitaxel-loaded conventional poly(anhydride) nanoparticles (PTX-NP)**

Briefly, 10 mg of PTX were dispersed in 5 ml of acetone containing 100 mg PVM/MA and incubated for 1 hour under magnetic stirring at room temperature. Then, nanoparticles were formed by the addition of 10 ml of ethanol followed by the addition of 10 ml of an aqueous solution containing glycine (50 mg) and disodium edetate (20 mg). The resulting nanoparticles were purified and lyophilised as described above.

### **2.2.3. Poly(anhydride) nanoparticles fluorescently labelled with RBITC**

For bioadhesive studies, conventional (NP) and pegylated nanoparticles were fluorescently labelled with RBITC [27]. For this purpose, nanoparticles were prepared as described above in the absence of paclitaxel and incubated with 1.25 mg RBITC at room temperature for 5 min. After adsorption of the marker, the nanoparticles were purified by centrifugation and, finally, freeze-dried.

For the identification the following abbreviations were used: NP (conventional or naked nanoparticles), NP2 (with PEG 2000), NP6 (with PEG 6000) and NP10 (with PEG 10000).

## **2.3. Characterization of nanoparticles**

The mean hydrodynamic diameter and the zeta potential of nanoparticles were determined by photon correlation spectroscopy (PCS) and electrophoretic laser Doppler anemometry, respectively, using a Zetamaster analyzer system (Malvern Instruments, UK). For this purpose, samples were diluted with deionised water and measured at 25 °C with a scattering angle of 90°.

The amounts of PEG associated with the nanoparticles were determined by quantification of the excipient in the supernatants collected from the purification step of nanoparticles using HPLC coupled to an Evaporative Light Scattering Detector (ELSD) [30]. Similarly, the poly(anhydride) content of nanoparticles was determined using the same HPLC-ELSD experimental conditions [30]. The yield of the nanoparticle preparation process was determined by gravimetry from freeze-dried samples as described previously [31].

The amount of RBITC loaded in the nanoparticles was determined by colorimetry at wavelength 540 nm after degradation with NaOH 0.1 N (Labsystems iEMS Reader MF, Finland) [27]. The quantity of loaded RBITC was estimated as a difference between its initial concentration and the concentration found after total hydrolysis of nanoparticles in 0.1 N NaOH. For the calculations standard curve of RBITC prepared in 0.1 N NaOH medium was used (concentration range of 4-30 µg/ml;  $r > 0.999$ ).

## 2.4. PTX analysis

The amount of PTX loaded into nanoparticles was quantified by HPLC [32]. The chromatographic system was an Agilent 1100 series (Waldborn, Germany), coupled with a UV diode array detection system. Data were analyzed using the Chemstation G2171 program (B.01.03). The separation of PTX was carried out at 30°C on a reversed-phase 150 x 3 mm C18 Phenomenex Gemini column (particle size 5 µm). The mobile phase, pumped at 0.5 ml/min, was 50:50 phosphate buffer (0.01 M, pH=2) - acetonitrile and effluent was monitored with UV detection at 228 nm. Docetaxel (DCX) was used as internal standard. Under these conditions the run time was 14 min and paclitaxel and docetaxel eluted at 6.1 min and 7.8 min, respectively. PTX and DCX stock solutions in ethanol were refrigerated and calibration curves were designed over the range 80–7000 ng/ml ( $r^2 > 0.999$ ). The limit of quantification was calculated to be 40 ng/ml.

For analysis, nanoparticles were digested with DMSO (1:5 v/v). The samples were transferred to auto-sampler vials, capped and placed in the HPLC auto sampler. Then, 10 µL aliquot was injected onto HPLC column. Each sample was assayed in triplicate and results were expressed as the amount of PTX (in µg) per mg nanoparticles. Similarly, the encapsulation efficiency (E.E.) was calculated as follows:

$$\text{E.E. (\%)} = (Q_{\text{associated}}/Q_{\text{initial}}) \times 100 \quad [\text{Eq. 1}]$$

where  $Q_{\text{initial}}$  was the initial amount of PTX that it was supposed to be added per mg of polymer that form the NP and  $Q_{\text{associated}}$  was the amount of PTX in digested nanoparticles, which was calculated from the HPLC measurements.

## 2.5. Permeation assays in Ussing chambers

The studies were performed after approval by the responsible Ethical Committee of the University of Paris-Sud (agreement number A92-019-01) in strict accordance with the European legislation in animal experiments.

### 2.5.1. Permeation experiments

Ussing chambers were used to evaluate the permeability of paclitaxel in fresh intestinal tissue when loaded in pegylated-poly(anhydride) nanoparticles. For this purpose, the methodology and terminology used in this work were those proposed previously [33]. Jejunum from fresh small intestine of sacrificed male Wistar rats (250 g; Charles River, Paris) was excised, rinsed with chilled physiological saline solution (NaCl 0.9%) and cut into segments of 2-3 cm length. Sections containing Peyer's patches were discarded.

Jejunum portions were mounted in Ussing chambers (the intestinal surface tested was 1 cm<sup>2</sup>) and bathed with PBS at pH 7.4 containing glutamine 0.2 M. The system was maintained at constant temperature and continuously oxygenated with O<sub>2</sub>/CO<sub>2</sub> (95%/5%).

In the receptor compartment, 0.1% (w/v) HPCD was also included as paclitaxel solubilising agent. Finally, after equilibration at the temperature of the



experiment (4°C or 37°C) for 30 min, the formulation to be tested was added to the donor compartment. For this purpose, nanoparticle batches containing 2 mg paclitaxel were resuspended in 300 µl of PBS (pH 7.4) prior to the addition to the donor chamber. Control tests were carried out with the same dose of PTX (2 mg) included in Taxol® and poly (anhydride) nanoparticles.

At pre-set time intervals, aliquots of 200 µL were recovered from the receptor chamber and replaced with the same volume of fresh medium pre-equilibrated at the experimental temperature conditions (4°C or 37°C). Samples (200 µl) were also taken from the donor chamber at the beginning and at the end of the experiment to monitor any changes in donor drug concentrations during the experiment and to safeguard mass balance. The samples were immediately frozen and stored at -20°C until analysis.

PTX content was determined by HPLC-UV as described above. Three tissue portions from three different animals were used to evaluate each formulation. The experiments were repeated on different days.

The cumulative amount of paclitaxel permeating in the mucosal-to-serosal (M to S, absorptive, or apical to basolateral) or serosal-to-mucosal (S to M, secretory, or basolateral to apical) direction was calculated and plotted against time. Also, the influence of different parameters (such as the temperature, the inhibition of the bioadhesion capacity of nanoparticles or the inhibition of P-gp with verapamil) on the permeability of intestinal tissue to paclitaxel was also studied.

In order to determine the influence of the bioadhesive capacity of nanoparticles on the absorption of paclitaxel, permeation studies were repeated avoiding the physical contact between the nanoparticles and the intestinal mucosa. In practice, a semi-permeable cellulose membrane (cut-off: 100,000 g/mol) was placed in the donor chamber at the surface of the luminal side of the intestinal mucosa. Further, the influence of the presence of verapamil on the permeability of paclitaxel was studied by adding 0.2 mM of this calcium blocker to the PBS solution in which the paclitaxel formulations were dispersed.

For comparisons, the following parameters were calculated: the apparent permeability coefficient (P<sub>app</sub>), the absorption enhancement ratio (R) and the efflux ratio (Er).

The apparent permeability coefficient (P<sub>app</sub>) was calculated using the following equation:

$$P_{app} = (dQ/dt) \times (1/C_0 A) \quad [\text{Eq. 2}]$$

where dQ/dt was the flux of PTX from the donor to receptor compartment of the mucosa, C<sub>0</sub> was the initial concentration of PTX in the donor compartment and A was the area of the membrane formed by the intestinal tissue.

The values of P<sub>app</sub> were calculated between 30 and 90 min after addition of the PTX formulation in all experiments, in order to standardize the calculations.

The absorption enhancement ratio (R) was calculated from P<sub>app</sub> values as follows:

$$R = P_{app} (\text{sample}) / P_{app} (\text{control}) \quad [\text{Eq. 3}]$$

where P<sub>app</sub> (sample) was the apparent permeability of jejunum to paclitaxel when included in the formulation tested and P<sub>app</sub> (control) was the apparent permeability to the drug when included in the reference formulation (Taxol®).

Finally, the efflux ratio ( $E_r$ ) was calculated as the ratio from the mean  $P_{app}$  measured from serosal-to-mucosal transport (S to M) and the mean measured from mucosal-to-serosal transport (M to S):

$$E_r = P_{app} \text{ S-M} / P_{app} \text{ M-S} \quad [\text{Eq. 4}]$$

### 2.5.2. Measurement of electrical parameters

Electrical parameters were also recorded to determine the tissue viability and the opening of tight junctions during the experiment. Transmucosal potential difference (PD) was continuously recorded between two KCl saturated agar bridges connected to an MDVC – 2C voltage clamp (Titis Bussines Corporation, Paris, France) via calomel electrodes filled with saturated KCl solution. Potential difference was short-circuited through the experiment by a short-circuit current ( $I_{sc}$ ) via agar bridges placed in each half-cell, and adapted to platinum electrodes connected to an automatic MDVC – 2C voltage clamp (Titis Bussines Corporation, Paris, France). Delivered  $I_{sc}$  (short – circuited current) was corrected for fluid resistance and recorded at pre – set times. The transmucosal electrical resistance (TEER) was calculated from the Ohm's law:

$$\text{TEER} = \text{PD} / I_{sc} \quad [\text{Eq. 5}]$$

where PD was the transmucosal potential difference and  $I_{sc}$  was the potential short circuited current.

Only tissues showing  $\text{PD} > 2.10^{-3} \text{ V}$  and  $I_{sc} > 40.10^{-6} \text{ A/cm}^2$  after 30 min equilibration were retained for the study. As a further test of the viability of the tissues, bumetanide DMSO stock solution (0.01 M) was added in the serosal compartment at the conclusion of the experiment. If there was no decrease in  $I_{sc}$ , damages in the tissue were suspected and samples collected from the corresponding chambers were discarded.

### 2.6. In vivo bioadhesive study

The bioadhesion study was carried out using a protocol described previously [31], after approval by the responsible Committee by the University of Navarra (Ethical and Biosafety Committee for Research on Animals; protocol 078-07), in line with the European legislation on animal experiments (86/609/EU).

Each animal received a single oral dose of 1 ml aqueous suspension containing 10 mg of the nanoparticles loaded with RBITC (approximately 45 mg particles/kg body weight). The animals were sacrificed by cervical dislocation one and three hours post-administration. The abdominal cavity was opened and the stomach, small intestine and cecum were removed, opened lengthwise along the mesentery and rinsed with phosphate saline buffer (pH 7.4). Further, the stomach, small intestine and cecum were digested in 3 N NaOH for 24 h. RBITC was extracted from the digested samples by addition of methanol, vortexed for 1 min and centrifuged at 4,000 rpm for 10 min. The samples were then analysed by spectrofluorimetry at  $\lambda_{ex}$  540 nm and  $\lambda_{em}$  580 nm (GENios Tecan, Austria) to estimate the fraction of adhered nanoparticles on the mucosa. For calculations, standard curves of RBITC were prepared by addition of RBITC-solutions in 3 N NaOH (0.5-10  $\mu\text{g/ml}$ ) to tissue segments following the same treatment steps ( $r > 0.996$ ).

### 2.7. Pharmacokinetic study of paclitaxel in rats

Animal experiments were performed according to the policies and guidelines of the responsible Committee of the University of Navarra in line with the



European legislation on animal experiments (86/609/EU) and following a protocol approved by the Ethic Committee of the University of Navarra (protocol number 076-06).

### **2.7.1. Administration of PTX-loaded pegylated nanoparticles to rats**

Male Wistar rats (average weight 225 g) (Harlan, Spain) were housed under normal conditions with free access to food and water. The animals were placed in metabolic cages and fasted overnight to prevent coprophagia but allowing free access to water.

For the pharmacokinetic study, the rats were divided at random in seven groups (n=6). The first group received intravenously by the vein of the tail 10 mg/kg of paclitaxel as Taxol® (commercial formulation) diluted with PBS until a final volume of 500 µl. The other groups of animals received paclitaxel (10 mg/kg) in different formulations by oral administration: (i) Taxol®; (ii) PTX-NP2; (iii) PTX-NP6; (iv) PTX-NP10 and (v) PTX-NP. All the animals received orally a total volume of 1 ml of either Taxol diluted with saline or nanoparticles dispersed in water just before the administration.

After administration, blood samples of 300 µl were collected at different times post-administration. EDTA was employed as anticoagulant. The volemia was recovered via intraperitoneal with an equal volume of normal saline solution preheated at body temperature. Blood samples were centrifuged for 10 min at 10,000 rpm and the supernatant plasma fraction was stored at -80°C until HPLC analysis.

### **2.7.2. HPLC quantification of paclitaxel in plasma samples**

The amount of paclitaxel was determined in plasma by HPLC as described above. Calibration curves were used for the conversion of the PTX/DCX chromatographic area to the concentration. Calibrator and quality control samples were prepared by adding appropriate volumes of standard PTX ethanolic solution to drug free plasma. Calibration curves were designed over the range 40–3200 ng/ml ( $r^2 > 0.999$ ). An aliquot (100 µl) of plasma sample was mixed with 25 µl of internal standard solution (docetaxel, 4 µg/ml in methanol, previously evaporated). After vortex mixing, liquid-liquid extraction was accomplished by adding 4 ml of tert-butylmethylether following vortex gentle agitation (1 min). The mixture was centrifuged for 10 min at 5,000 rpm, and then, the organic layer was transferred to a clean vial and evaporated until dry (Savant, Barcelona, Spain). Finally, the residue was dissolved in 125 µl of reconstitution solution (acetonitrile – phosphate buffer 0.01M pH=2; 50/50 v/v) and transferred to auto-sampler vials, capped and placed in the HPLC auto sampler. A 100 µl aliquot of each sample was injected onto the HPLC column.

The limit of quantification was calculated as 80 ng/mL with a relative standard deviation of 5.2%. Accuracy values during the same day (intra-day assay) at low, medium and high concentrations of PTX were always within the acceptable limits (less than 5%) at all concentrations tested.

### **2.7.3. Pharmacokinetic data analysis**

The pharmacokinetic analysis of concentration-time data, obtained before the administration of the different PTX formulations, was analyzed using a noncompartmental model using WinNonlin 5.2 software (Pharsight Corporation, Mountain View, EEUU). The pharmacokinetic parameters estimated were: the maximal plasmatic concentration ( $C_{max}$ ), time in which the maximum concentration was reached ( $T_{max}$ ), the half-life of the terminal phase ( $t_{1/2}$ ), the area under the concentration-time curve from time 0 to  $\infty$  ( $AUC_{0-\infty}$ ) and the

mean residence time (MRT). The relative bioavailability of paclitaxel ( $F_R$ ) was calculated according to the following equation:

$$F_R = (AUC_{\text{oral}} / AUC_{\text{i.v.}}) \times 100 \quad [\text{Eq. 6}]$$

where  $AUC_{\text{oral}}$  was the area under the concentration versus time curve after oral administration and  $AUC_{\text{i.v.}}$  was the AUC for Taxol<sup>®</sup> administered by the i.v. route.

## 2.8. Statistical analysis

The permeability values and pharmacokinetic results were expressed as mean values  $\pm$  SD. The nonparametric Kruskal-Wallis followed by Mann-Whitney U-test with Bonferroni correction was used to investigate statistical differences. In all cases,  $p < 0.05$  was considered to be significant. All calculations were performed using SPSS<sup>®</sup> statistical software program (SPSS<sup>®</sup> 15.0, Microsoft, USA).

## 3. Results

### 3.1. Preparation and characterisation of PTX-PEG poly(anhydride) nanoparticles

Nanoparticles were prepared after the incubation of a mixture of poly(anhydride) and PEG with the anticancer drug. Then the polymer was desolvated by the addition of ethanol and water and the resulting nanoparticles were freeze-dried after purification. For the optimization of paclitaxel-loaded pegylated nanoparticles, the effect of the bulk concentration of paclitaxel (expressed as the ratio between the drug and the polymer) on the drug loading was evaluated. Figure 1 shows the evolution of the paclitaxel loading in the different pegylated nanoparticles as a function of the PTX/poly(anhydride) ratio. Interestingly, for all the different formulations tested, by increasing the amount of the bulk paclitaxel, the drug loading increased sharply until a PTX/poly(anhydride) ratio of 0.1. However, at ratios higher than 0.1, aggregation of the nanoparticle was observed.

At a PTX/poly(anhydride) ratio of 0.1, the total amount of encapsulated paclitaxel was similar for the different pegylated nanoparticles (irrespective of the MW of PEG) and close to 150  $\mu\text{g}$  drug per mg nanoparticles. For control nanoparticles, the maximum drug loading was calculated to be about 80  $\mu\text{g}$  of PTX per mg/nanoparticles.

The main physico-chemical characteristics of PTX-PEGylated poly(anhydride) nanoparticles used in this work are summarised in Table 1. Control nanoparticles (PTX-NP) displayed a mean size of  $177 \pm 3$  nm and a zeta potential close to -45 mV. Pegylation of poly(anhydride) nanoparticles did not modified the mean particle size; although, the zeta potential was found to be slightly lower than that of control nanoparticles. Furthermore, the yield of the preparative process was similar for all the formulations and close to 60-65%. Finally, the PTX encapsulation efficiencies were found to be more than 2-times higher for pegylated nanoparticles than for control ones. Overall all the pegylated nanoparticles displayed similar physico-chemical characteristics, independently of the MW of the PEG used for pegylation.

### 3.2. Permeability studies in Ussing chambers

The transport and permeability of paclitaxel through the jejunum mucosa of rats was determined "ex vivo" in Ussing chambers. Table 2 summarizes the

apparent permeability coefficients,  $P_{app}$  in cm/s, and the absorption enhancement ratios (R) of paclitaxel calculated for the different formulations tested.

In the M-S direction, the apparent permeability of paclitaxel when formulated as Taxol® was found to be very low (about  $1.2 \times 10^{-6}$  cm/s). For the control formulation of paclitaxel loaded in conventional nanoparticles (PTX-NP), the apparent permeability was slightly higher than for Taxol® (about  $2.1 \times 10^{-6}$  cm/s). On the contrary, when PTX was incorporated in pegylated nanoparticles (PTX-NP2, PTX-NP6 and PTX-NP10) the intestinal permeability of paclitaxel increased between 3 and 7 times compared with the commercial formulation. Interestingly, the permeability of PTX was significantly higher when the drug was loaded in nanoparticles pegylated with either PEG 2000 or PEG 6000 than when decorated with PEG 10000 ( $p < 0.005$ ).

When the apparent intestinal permeability of PTX (Taxol®) was studied in the secretory direction (S-M), the paclitaxel permeability was found to be much higher than that observed in the absorptive direction (M-S). Thus, for Taxol®, the absorption enhancement ratio (R) was about 27 times higher than when evaluated in the mucosal-to-serosal direction. Similarly, when drug was formulated in pegylated nanoparticles (PTX-NP2), the  $P_{app}$  value was found to be about  $22 \times 10^{-6}$  cm/s, which represented an efflux ratio of about 2.5.

On the other hand, it is well known that paclitaxel is substrate of the P-glycoprotein. Thus, when P-glycoprotein was inhibited with verapamil, the permeability of paclitaxel was 3-times higher than in normal conditions (see Table 2). On the contrary, when contact between PTX-NP2 and the intestinal tissue was hampered by the presence of a semi-permeable membrane, paclitaxel was unable to be absorbed through the intestinal tissue and the apparent permeability was very low ( $P_{app} = 0.3 \times 10^{-6}$  cm/s).

### 3.3. In vivo bioadhesion study

In vivo bioadhesive studies were performed using RBITC-labelled nanoparticles (Figure 2). Thus, 1 h post-administration, conventional nanoparticles (NP) displayed a higher ability to interact with the stomach mucosa than pegylated nanoparticles. On the contrary, in the small intestine, nanoparticles pegylated with either PEG 2000 (NP2) or PEG 6000 (NP6) interacted in a significantly higher extent with the mucosa than NP or NP10 ( $p < 0.01$ ). In fact, for NP2 and NP6, around 23% of the given dose was found adhered to the small intestine mucosa, whereas only 12% for NP and 9% for NP10 was quantified in this gut region.

On the other hand, 3-h post-administration, the adhered fraction of nanoparticles in the small intestine was similar for the three pegylated nanoparticles (between 23-27% of the given dose). These amounts were significantly higher than for NP ( $p < 0.01$ ). In the stomach, the amount of nanoparticles found were much lower and similar for all the formulations tested (less than 5 % of the given dose).

### 3.4. Pharmacokinetics of paclitaxel in rats

Figure 3 shows the paclitaxel plasma concentration versus time profile after intravenous administration of Taxol® at a dose of 10 mg/kg in rat. As expected, the drug plasma concentration rapidly decreased with time in a biphasic way and the data were adjusted by noncompartmental model. The peak plasma

concentration ( $C_{max}$ ) of paclitaxel was about 204  $\mu\text{g/ml}$ . The mean values obtained for AUC and half-life ( $T_{1/2z}$ ) were 81  $\mu\text{g ml}^{-1} \text{h}^{-1}$  and 2.6 h, respectively. The MRT was 1.7 h (Table 3).

Figure 4 shows the plasma concentration versus time profile after oral administration of paclitaxel (single dose of 10 mg/kg) included in the different nanoparticle formulations. When commercial Taxol<sup>®</sup> was administered to rats by the oral route, PTX plasmatic levels detected were very low; always under the quantification limit of the HPLC technique (80 ng/ml). On the contrary, when paclitaxel was loaded in pegylated poly(anhydride) nanoparticles, sustained plasma levels of the anticancer drug were observed. These plasma curves were characterised by increasing amounts of paclitaxel in plasma during the first 3-6 h followed by a step in which the drug plasma concentration was maintained at high and constant levels until 10 h (for PTX-NP10) or 48 h post administration (for PTX-NP2 and PTX-NP6). During this second step, it was observed that PTX-NP2 displayed higher levels of PTX than PTX-NP6. Finally, the paclitaxel plasma concentration decreased rapidly; although, 72 h post-administration, quantifiable amounts of drug were still found. For conventional nanoparticles, in spite of higher than for Taxol<sup>®</sup>, the plasma levels of paclitaxel remained low and close to the defined therapeutic concentration (85 ng/ml; [25]).

Table 3 summarizes the pharmacokinetic parameters estimated with a non-compartmental analysis of the experimental data obtained after the oral administration of the different PTX formulations to rats. As seen in Table 3, the paclitaxel  $C_{max}$  for the nanoparticle formulations were found to be about 100-120 times lower than that of the drug formulation administered by the i.v. route. On the contrary,  $C_{max}$  for pegylated nanoparticles was about 9-14 fold higher than that of conventional nanoparticles. Within the different pegylated nanoparticles, the rank order of the mean maximum plasma drug concentration among the different formulations was as follows: PTX-NP2 = PTX-NP6 > PTX-NP10 ( $p < 0.05$ ). Similarly, the AUC values were found to be dependent on the molecular weight of PEG used in the formulation. For PTX-NP2 and PTX-NP6 oral formulations, AUC values were 4.3 and 2.5-folds respectively higher than the AUC obtained for PTX-NP10 administered at the same dose of the drug.

In addition, the mean residence time (MRT) of the drug in plasma and the  $t_{1/2}$  were found higher when paclitaxel was administered in the nanoparticle formulations by the oral route than when administered as Taxol<sup>®</sup> by the i.v. route. For PTX-NP2 and PTX-NP6, the MRT of paclitaxel was higher than for PTX-NP10. On the contrary, PTX-NP10 showed a terminal elimination half-life of paclitaxel of about 4.6 and 3.1-fold higher than for PTX-NP6 and PTX-NP2 respectively.

Finally, the relative oral bioavailability of paclitaxel delivered in nanoparticles was calculated to be 70% for PTX-NP2, 40% for PTX-NP6 and 16% in case of PTX-NP10. For non pegylated nanoparticles the oral bioavailability was found to be only 9%.

#### 4. Discussion

Paclitaxel, classified as class IV drug of the biopharmaceutical classification system, shows a very low bioavailability when administered by the oral route. This fact is due to both its low aqueous solubility ( $\log P = 3.5$ ) and low intestinal permeability mainly due the effect of the P-glycoprotein and cytochrome P450 (i.e. CYP3A4) expressed in the epithelial enterocytes [16, 34, 35].



In order to overcome these drawbacks and increase the intestinal permeability of paclitaxel one possible strategy may be the combination between bioadhesive nanoparticles and excipients capable to inhibit the activity of Pgp and/or the cytochrome P450. In this context, the use of pegylated poly(anhydride) nanoparticles may be of interest for this purpose. These nanoparticles have shown a high ability to cross the mucus layer and reach the surface of the enterocytes [27]. In addition, PEG has shown a moderate inhibitory effect of both P-gp and CYP3A4 [36].

Pegylated nanoparticles were prepared by a simple incubation of paclitaxel, polyethylenglycol and the poly(anhydride) in an acetone medium followed by the desolvation of the polymers with ethanol and water. During the desolvation step glycine was added to promote the encapsulation of paclitaxel in the resulting nanoparticles. The exact mechanism by which this amino acid augmented the paclitaxel loading has not been yet elucidated; although, glycine has been described as an auxiliary substance to promote the solubility of lipophilic compounds (i.e. dehydroepiandrosterone) [37]. In any case, this increase in the encapsulation efficiency of paclitaxel was particularly impressive for conventional nanoparticles, in which the addition of glycine enabled us to increase the drug loading from 0.3  $\mu\text{g}/\text{mg}$  nanoparticle (not shown) to close to 80  $\mu\text{g}/\text{mg}$  (Table 1). Interestingly, the amount of paclitaxel loaded in pegylated nanoparticles was not dependent on the MW of the PEG employed for pegylation and was calculated to be about 150  $\mu\text{g}/\text{mg}$  nanoparticles (about 15% w/w). This fact is in agreement with previous results published by Bartoli and collaborators (1990) [38] who described a significant increase of paclitaxel loading in pegylated liposomes, in comparison with plain liposomes.

Concerning the studies of permeability of paclitaxel in Ussing chambers, the differences in the drug permeation rates observed in the mucosal-to-serosal direction vs. serosal-to-mucosal orientation is a classical indication that efflux pump is involved in the transport of the drug across the jejunum tissue [39]. The asymmetric permeation found for free paclitaxel (Taxol<sup>®</sup>) ( $P_{\text{app M-S}}$  1.2 vs.  $P_{\text{app S-M}}$  32.1; Table 2) and an efflux ratio (calculated by eq. 4) of about 27, confirmed the presence of an active mechanism, such as apically polarized efflux proteins, for which paclitaxel is a very good substrate [40]. The involvement of P-glycoprotein in the intestinal absorption of paclitaxel included in pegylated nanoparticles (PTX-NP2) was confirmed by the addition of the calcium blocker verapamil (a well known inhibitor of the P-gp efflux pump [14]) at a concentration of 0.2 mM on the apical side. The apparent permeability coefficient of paclitaxel was found to be 3-fold higher when verapamil was added to the donor compartment containing the PTX-NP2 formulation.

On the other hand, when PTX was included in pegylated nanoparticles, the permeability of the anticancer drug significantly increased as compared with the controls (Taxol<sup>®</sup> and PTX-NP), confirming a significant decrease in the efflux transport of paclitaxel which can be considered as a clear evidence of inhibition of the active secretory transport of paclitaxel by these pegylated carriers. However, this positive effect of pegylated nanoparticles on the permeability of paclitaxel appeared to be influenced by the molecular weight of the PEG used. In fact, the apparent permeability of paclitaxel when loaded in nanoparticles pegylated with either PEG 2000 or PEG 6000 was 2.5-times higher than when loaded in nanoparticles pegylated with PEG10000. Interestingly, nanoparticles pegylated with either PEG 2000 or PEG 6000 displayed higher bioadhesive



properties than nanoparticles pegylated with PEG 10000 (see Figure 2). In any case, the importance of the bioadhesive interactions between nanoparticles and the mucosa for the absorption of paclitaxel was highlighted by the introduction of a membrane between the jejunum and the suspension of nanoparticles. Under these experimental conditions, paclitaxel was not able to pass through the jejunum tissue and the apparent permeability was found to be 28-fold lower than under normal conditions. This observation confirmed that the close contact between nanoparticles and the mucosa tissue is a key point to enhance the absorption of paclitaxel and is in agreement with previous results in which paclitaxel was loaded in bioadhesive cyclodextrin-poly(anhydride) nanoparticles [32].

For the pharmacokinetic study, a single-dose of 10 mg/kg was selected. When Taxol<sup>®</sup> was administered by the intravenous route, the profile of the curve was biphasic (Figure 3) and similar to that published previously. From the plasma curve, the mean AUC and the terminal half life ( $t_{1/2z}$ ) for paclitaxel was calculated to be about 81  $\mu\text{g/h ml}$  and 2.6 h. These values were consistent with data previously reported of paclitaxel administered in rats at the same dose [21, 25, 41, 42]. On the contrary, when Taxol<sup>®</sup> was administered by the oral route, the plasma levels of paclitaxel were negligible (not shown) and it was not possible to calculate the relative oral bioavailability ( $F_r$ ) of paclitaxel when formulated in the commercial formulation. In any case,  $F_r$  of paclitaxel when orally administered has been reported to be between 2 and 10.5% [15, 25, 43].

When paclitaxel was loaded in pegylated nanoparticles and orally administered to rats, the plasma levels of paclitaxel were high and prolonged in time (Figure 4). However some differences in the profile of the curves were found. Thus, the peak of the maximum concentration ( $C_{\text{max}}$ ) of paclitaxel in plasma was found to be dependent on the MW of PEG associated with the nanoparticles. In fact, the  $C_{\text{max}}$  value decreased by increasing the MW of the PEG used for the pegylation of nanoparticles. On the other hand, for PTX-NP2 and PTX-NP6, the levels of paclitaxel in plasma remained high and constant from 48 h; although, the plateau of paclitaxel concentration was higher for PTX-NP2 than for PTX-NP6. On the contrary, the profile of the curve for PTX-NP10 was characterised by a slow decrease of paclitaxel plasma levels after from the  $C_{\text{max}}$  of the curve till 32 h post-administration. From these curves, the relative oral bioavailability of paclitaxel was calculated to be about 70% for PTX-NP2, 40% for PTX-NP6 and 16% in the case of PTX-NP10, whereas for non pegylated nanoparticles (PTX-NP)  $F_r$  was about 9%. These results are in agreement with data obtained from the ex vivo studies in Ussing chambers (see Table 2) in which PTX-NP2 and PTX-NP6 offered the highest values of permeability across the jejunum of animals. Overall all of these results confirm that this type of nanoparticles may be of interest to reduce the impact of the efflux pump P-gp and the metabolism effect by cytochrome P450 and, hence, create favourable conditions for enhancing the absorption of paclitaxel.

Overall, all the relative bioavailability data obtained with the different pegylated formulations was high. For PTX-NP2, the oral bioavailability of paclitaxel was found to be of the same order that those previously reported with cyclodextrin-poly(anhydride) nanoparticles. These carriers offer a paclitaxel  $F_r$  of about 80% when poly(anhydride) nanoparticles were loaded with the anticancer drug as complex with either hydroxypropyl- $\beta$ -cyclodextrin or  $\beta$ -cyclodextrin [44]. Similar bioavailability levels were also reported by Khandavilli and Panchagnula (2007)

[42] by incorporating paclitaxel in a nanoemulsion formulation of a mixture of labrasol and vitamin E-TPGS (3:1).

However, in our case, particularly interesting resulted the performance of pegylated nanoparticles to prolong the therapeutic plasma levels of paclitaxel for at least 48 h in rats. It is interesting to note that a such plasma profile, characterised by relatively stable drug blood levels, would provide a more consistent therapeutic effect than frequent doses of short acting medications. In addition, fewer peaks and valleys oscillations may result in fewer side effects. For PTX-NP2 and PTX-NP6, the paclitaxel plasma concentration were maintained in a high and constant level from 3 to 48 h post-administration with values till around 20-fold higher than the reported therapeutic range of 0.1  $\mu\text{mol/L}$  (equivalent to 85 ng/ml [25, 45]). This phenomenon has also been observed for cyclodextrin-poly(anhydride) nanoparticles [44] and nanoemulsions [42]. However, in these cases, the persistence of high paclitaxel plasma levels was restricted to a period of time of 24 h or 18 h, respectively. The long persistence of paclitaxel in plasma when formulated with pegylated nanoparticles was also confirmed by the calculated MRT data (Table 3). MRT values of paclitaxel when formulated as PTX-NP2 and PTX-NP6 (26 h) were found to be 18 times higher than the MRT calculated for paclitaxel i.v. administered as Taxol<sup>®</sup> (1.7 h).

All of these results appear to be related with the bioadhesive properties of the different pegylated nanoparticles. Thus, pegylation of nanoparticles with either PEG 2000 or PEG 6000 yielded carriers capable to develop more appropriate adhesive interactions than nanoparticles pegylated with PEG 10000 (see Figure 2). This finding may be due to a lower interaction between the components of the mucus layer of nanoparticles pegylated with either PEG 2000 or PEG 6000 than with PEG 10000. In the past we demonstrated that the adhesive interactions of conventional poly(anhydride) nanoparticles were mainly restricted to the mucus layer [46]. When these nanoparticles were pegylated with PEG 2000, the PEG chains adopted a “brush” conformation that would facilitate their diffusion across the mucus protective layer [27, 47]. A similar behaviour can be expected from nanoparticles pegylated with PEG 6000. On the contrary, for nanoparticles pegylated with PEG 10000, the disposition of the PEG chains covering the surface of nanoparticles would favour the interpenetration and interaction with the mucus fibers [48]. This explanation is in agreement with Lai and co-workers who hypothesised that coating particles with PEG, may reduce particle–mucus adhesive interactions if the molecular mass of PEG was too low (< 10 kDa) to support adhesion by polymer interpenetration [49].

As a result pegylated nanoparticles with either PEG 2000 or 6000 would be located at the surface of the absorptive membrane for a long period of time and during this period they would release their content. The presence of PEG in close contact with the surface of mature enterocytes would facilitate the inhibition of the P-gp and the cytochrome P450 and, thus, the absorption of paclitaxel as suggested by permeation experiments. In any case, these hypothetical processes of interactions between nanoparticles and the mucosa require further investigations.

In summary, this study has demonstrated the capability of pegylated poly(anhydride) nanoparticles to increase the oral permeability and to prolong for at least 48 h sustained and therapeutic plasma levels of paclitaxel in rats.

These effects would be related with the diffusion abilities of these carriers through the mucus layer and, probably, with the reported inhibitory effect of PEG on P-gp and P450 cytochrome. Particularly interesting were the results obtained with nanoparticles pegylated with PEG 2000 and PEG 6000 which provided a relatively oral bioavailability of paclitaxel in rat of about 70% and 40%, respectively.

### **Acknowledgements**

This work was supported by a collaborative French–Spanish project (PICASSO grant, numbers HF2007-0061, 17121NG) and by the Ministry of Science and Innovation in Spain (projects SAF2008-02538 and PCT-090100-2007-27). Virginia Zabaleta was also financially supported by a grant from the Department of Education of the Gobierno de Navarra in Spain.

### **References**

- [1] W.S. Fang, X.T. Liang, Recent progress in structure activity relationship and mechanistic studies of taxol analogues, *Mini Rev. Med. Chem.* 5 (2005) 1-12.
- [2] G. Samaranayake, K.A. Neidigh, D.G. Kingston, Modified taxols, 8. Deacylation and reacylation of baccatin III, *J. Nat. Prod.* 56 (1993) 884-898.
- [3] S.B. Horwitz, Mechanism of action of taxol, *Trends Pharmacol. Sci.* 13 (1992) 134-136.
- [4] J.A. Sparano, M. Wang, S. Martino, V. Jones, E.A. Perez, T. Saphner, A.C. Wolff, G.W. Sledge, W.C. Wood, N.E. Davidson, Weekly paclitaxel in the adjuvant treatment of breast cancer, *N. Engl. J. Med.* 358 (2008) 1663–1671.
- [5] M. Montana, C. Ducros, P. Verhaeghe, T. Terme, P. Vanelle, P. Rathelot, Albumin-bound paclitaxel: the benefit of this new formulation in the treatment of various cancers, *J. Chemother.* 23 (2011) 59-66.
- [6] A. Sandler, R. Gray, M.C. Perry, J. Brahmer, J.H. Schiller, A. Dowlati, R. Lilienbaum, D.H. Johnson, Paclitaxel–carboplatin Alone or with bevacizumab for non–small-cell lung cancer, *N. Engl. J. Med.* 355 (2006) 2542-2550
- [7] M. Zhan, W.Y. Tao, S.H. Pan, X.Y. Sun, H.C. Jiang, Low-dose metronomic chemotherapy of paclitaxel synergizes with cetuximab to suppress human colon cancer xenografts, *Anti-Cancer Drug.* 20 (2009) 355–363.
- [8] P.S. Gill, A. Tulpule, B.M. Espina, S. Cabriales, J. Bresnahan, M. Ilaw, S. Louie, N.F. Gustafson, M.A. Brown, C. Orcutt, B. Winograd, D.T. Scadden, Paclitaxel is safe and effective in the treatment of advanced AIDS-related Kaposi’s sarcoma, *J. Clin. Oncol.* 17 (1999) 1876-1883.
- [9] M.R. Wenk, A. Fahr, R. Reszka, J. Seelig, Paclitaxel partitioning into lipid bilayers, *J. Pharm. Sci.* 85 (1996) 228–231.
- [10] A.K. Singla, A. Garg, D. Aggarwal, Paclitaxel and its formulations, *Int. J. Pharm.* 235 (2002) 179–192.
- [11] J.S. Kloover, M.A. den Bakker, H. Gelderblom, J.P. van Meerbeeck, Fatal outcome of a hypersensitivity reaction to paclitaxel: a critical review of premedication regimens, *Br. J. Cancer.* 90 (2004) 304-305.

- [12] S.C. Kim, H.J. Yoon, J.W. Lee, J. Yu, E-S. Park, S.C. Chi, Investigation of the release behaviour of DEHP from infusion sets by paclitaxel-loaded polymeric micelles, *Int J. Pharm.* 293 (2005) 303-310.
- [13] C.D. Scripture, J. Szebeni, W.J. Loos, W.D. Figg, A. Sparreboom, Comparative in vitro properties and clinical pharmacokinetics of paclitaxel following the administration of Taxol® and Paxene®, *Cancer Biol. Ther.* 4 (2005) 555-560.
- [14] C.M. Kruijtzter, J.H. Beijnen, J.H. Schellens, Improvement of oral drug treatment by temporary inhibition of drug transporters and/or cytochrome P450 in the gastrointestinal tract and liver: an overview, *Oncologist* 7 (2002) 516-530.
- [15] S. Peltier, J.M. Oger, F. Lagarce, W. Couet, J.P. Benoît, Enhanced oral paclitaxel bioavailability after administration of paclitaxel-loaded lipid Nanocapsules. *Pharm. Res.* 23 (2006) 1243-1250.
- [16] Y. Zhang, L.Z. Benet, The gut as a barrier to drug absorption: combined role of cytochrome P450 3A and P-glycoprotein, *Clin. Pharmacokinet.* 40 (2001) 159–168.
- [17] L.E. Broker, S.A. Veltkamp, E.I. Heath, B.C. Kuenen, H. Gall, L. Astier, S. Parker, L. Kayitalire, P.M. Lorusso, J.H. Schellens, G. Giaccone, A phase I safety and pharmacologic study of a twice weekly dosing regimen of the oral taxane BMS-275183, *Clin. Cancer Res.* 13 (2007) 3906-3912.
- [18] T.A. Brooks, H. Minderman, K.L. O'Loughlin, P. Pera, I. Ojima, M.R. Baer, R.J. Bernacki, Taxane-based reversal agents modulate drug resistance mediated by P-glycoprotein, multidrug resistance protein, and breast cancer resistance protein, *Mol. Cancer Ther.* 2 (2003) 1195-1205.
- [19] K.L. Hennenfent, R. Govindan, Novel formulations of taxanes: a review. Old wine in a new bottle?, *Ann. Oncol.* 17 (2006) 735-749.
- [20] M. Bayes, X. Rabasseda, J.R. Prous, Gateways to clinical trials, *Methods Find. Exp. Clin. Pharmacol.* 26 (2004) 53-84.
- [21] H. Li, M. Huo, J. Zhou, Y. Dai, Y. Deng, X. Shi, J. Massoud, Enhanced oral absorption of paclitaxel in N-deoxycholic acid-N, O-hydroxyethyl chitosan micellar system, *J. Pharm. Sci.* 99 (2010) 4543-4553.
- [22] Z.S. Bavindir, N. Yuksel, Characterization of niosomes prepared with various nonionic surfactants for paclitaxel oral delivery, *J. Pharm. Sci.* 99 (2010) 2049-2060.
- [23] G. Kim, S. Nie, Targeted cancer nanotherapy, *Mater. Today* 8 (2005) 28–33.
- [24] P. Gao, B.D. Rush, W.P. Pfund, T. Huang, J.M. Bauer, W. Morozowich, M.S. Kuo, M.J. Hageman, Development of a supersaturable SEDDS (S SEDDS) formulation of paclitaxel with improved oral bioavailability, *J. Pharm. Sci.* 92 (2003) 2386–2398.
- [25] S. Yang, R.N. Gursoy, G. Lambert, S. Benita, Enhanced oral absorption of paclitaxel in a novel self-microemulsifying drug delivery system with or without concomitant use of P-glycoprotein inhibitors, *Pharm. Res.* 21 (2004) 261–270.
- [26] B.D. Rege, J.P. Kao, J.E. Polli, Effects of nonionic surfactants on membrane transporters in Caco-2 cell monolayers, *Eur. J. Pharm. Sci.* 16 (2002) 237–246.

- [27] K. Yoncheva, E. Lizarraga, J.M. Irache, Pegylated nanoparticles based on poly(methyl vinyl ether-co-maleic anhydride): preparation and evaluation of their bioadhesive properties, *Eur. J. Pharm. Sci.* 24 (2005) 411-419.
- [28] E.D. Hugger, K.L. Audus, R.T. Borchardt, Effects of poly(ethylene glycol) on efflux transporter activity in Caco-2 cell monolayers, *J. Pharm. Sci.* 91 (2002) 1980-1990.
- [29] B.M. Johnson, W.N. Charman, C.J. Porter, An in vitro examination of the impact of polyethylene glycol 400, Pluronic P85, and vitamin E d-alpha-tocopheryl polyethylene glycol 1000 succinate on P-glycoprotein efflux and enterocyte-based metabolism in excised rat intestine, *AAPS PharmSci.* 4 (2002) E40.
- [30] V. Zabaleta, M.A. Campanero, J.M. Irache, An HPLC with evaporative light scattering detection method for the quantification of PEGs and Gantrez in PEGylated nanoparticles, *J. Pharm. Biomed. Anal.* 44 (2007) 1072-1078.
- [31] P. Arbos, M.A. Arangoa, M.A. Campanero, J.M. Irache, Quantification of the bioadhesive properties of protein-coated PVM/MA nanoparticles, *Int. J. Pharm.* 242 (2002) 129-136.
- [32] M. Agüeros, L. Ruiz-Gatón, C. Vauthier, K. Bouchemal, S. Espuelas, G. Ponchel, J.M. Irache, Combined hydroxypropyl- $\beta$ -cyclodextrin and poly(anhydride) nanoparticles improve the oral permeability of paclitaxel, *Eur. J. Pharm. Sci.* 38 (2009) 405-413
- [33] I. Bravo-Osuna, C. Vauthier, H. Chacun, G. Ponchel, Specific permeability modulation of intestinal paracellular pathway by chitosan-poly(isobutyl cyanoacrylate) core-shell nanoparticles, *Eur. J. Pharm. Biopharm.* 69 (2008) 436-444.
- [34] A.B. Dhanikula, R. Panchagnula, Localized paclitaxel delivery, *Int. J. Pharm.* 183 (1999) 85-100.
- [35] J.S. Woo, C.H. Lee, C.K. Shim, S-J. Hwang, Enhanced oral bioavailability of paclitaxel by coadministration of the P-glycoprotein inhibitor KR30031, *Pharm. Res.* 20 (2003) 24-30.
- [36] S.W. Wang, J. Monagle, C. McNulty, D. Putnam, H. Chen, Determination of P-glycoprotein inhibition by excipients and their combinations using an integrated high-throughput process, *J. Pharm. Sci.* 93 (2004) 2755-2767.
- [37] P.C. Mora, M. Cirri, S. Guenther, B. Allolio, F. Carli, P. Mura, Enhancement of dehydroepiandrosterone solubility and bioavailability by ternary complexation with alpha-cyclodextrin and glycine, *J. Pharm. Sci.* 92 (2003) 2177-2184.
- [38] M.H. Bartoli, M. Boitard, H. Fessi, H. Berial, J.P. Devissaguet, F. Picot, F. Puisieux, In vitro and in vivo antitumoral activity of free, and encapsulated taxol, *J. Microencapsul.* 7 (1990) 191-197.
- [39] M.V. Varma, R. Panchagnula, Enhanced oral paclitaxel absorption with vitamin E-TPGS: effect on solubility and permeability in vitro, in situ and in vivo, *Eur. J. Pharm. Sci.* 25 (2005) 445-453.
- [40] R. Jain, S. Agarwal, S. Majumdar, X. Zhu, D. Pal, A.K. Mitra, Evasion of P-gp mediated cellular efflux and permeability enhancement of HIV-protease inhibitor saquinavir by prodrug modification, *Int. J. Pharm.* 303 (2005) 8-19.
- [41] C.M. Kearns, L. Gianni, M.J. Egorin, Paclitaxel pharmacokinetics and pharmacodynamics, *Semin. Oncol.* 22 (1995) 16-23.



- [42] S. Khandavilli, R. Panchagnula, Nanoemulsions as versatile formulations for paclitaxel delivery: peroral and dermal delivery studies in rats, *J. Invest. Dermatol.* 127 (2007) 154-162.
- [43] T.K. Yeh, Z. Lu, M.G. Wientjes, J.L. Au, Formulating paclitaxel in nanoparticles alters its disposition, *Pharm. Res.* 22 (2005) 867-874.
- [44] M. Agüeros, V. Zabaleta, S. Espuelas, M.A. Campanero, J.M. Irache, Increased oral bioavailability of paclitaxel by its encapsulation through complex formation with cyclodextrins in poly(anhydride) nanoparticles, *J. Control. Release* 145 (2010) 2-8.
- [45] J.M. Meerum Terwogt, M.M. Malingre, J.H. Beijnen, W.W. ten Bokkel Huinink, H. Rosing, F.J. Koopman, O. van Tellingen, M. Swart, J.H. Schellens, Coadministration of oral cyclosporin A enables oral therapy with paclitaxel, *Clin. Cancer Res.* 5 (1999) 3379-3384.
- [46] P. Arbós, M.A. Campanero, M.A. Arangoa, M.J. Renedo, J.M. Irache, Influence of the surface characteristics of PVM/MA nanoparticles on their bioadhesive properties. *J. Control. Release* 89 (2003) 19-30.
- [47] K. Yoncheva, L. Guembe, M.A. Campanero, J.M. Irache, Evaluation of bioadhesive potential and intestinal transport of pegylated poly(anhydride) nanoparticles, *Int. J. Pharm.* 334 (2007) 156-165.
- [48] Y. Huang, W. Leobandung, A. Foss, N.A. Peppas Molecular aspects of muco- and bioadhesion: tethered structures and site-specific surfaces, *J. Control. Release* 65 (2000) 63-71.
- [49] S.K. Lai, D.E. O'Hanlon, S. Harrold, S.T. Man, Y-Y. Wang, R. Cone, J. Hanes, Rapid transport of large polymeric nanoparticles in fresh undiluted human mucus. *PNAS* 104 (2007) 1482-1487.

**Table 1.** Characterization of PTX-loaded pegylated poly (anhydride) nanoparticles. Data expressed as the mean  $\pm$  SD (n=8). PTX-NP: paclitaxel-loaded poly(anhydride) nanoparticles; PTX-NP2: paclitaxel loaded in nanoparticles pegylated with PEG 2000; PTX-NP6: paclitaxel loaded in nanoparticles pegylated with PEG 6000; PTX-NP10: paclitaxel loaded in nanoparticles pegylated with PEG 10000. PDI: polydispersion index.

Formulation	Size (nm)	PDI	Zeta Potencial (mV)	Yield (%)	PTX loading ( $\mu$ g/mg NP)	Encapsulation Efficiency (%)
PTX-NP	177 $\pm$ 3	0.038	-44.2 $\pm$ 7.1	62.2 $\pm$ 1.1	78.1 $\pm$ 3.2	38.2 $\pm$ 5.3
PTX-NP2	178 $\pm$ 4	0.154	-40.3 $\pm$ 1.1	60.1 $\pm$ 1.2	150.1 $\pm$ 5.2	88.3 $\pm$ 7.4
PTX-NP6	180 $\pm$ 5	0.173	-39.5 $\pm$ 4.2	63.8 $\pm$ 2.1	144.1 $\pm$ 3.1	78.1 $\pm$ 7.3
PTX-NP10	188 $\pm$ 2	0.136	-41.1 $\pm$ 1.3	63.1 $\pm$ 0.8	144.5 $\pm$ 6.4	74.9 $\pm$ 6.2

**Table 2.** Apparent intestinal jejunum permeability of paclitaxel under different experimental conditions as determined using the Ussing Chambers. Each value represents the mean  $P_{app} \pm$  S.D (n = 4). M-S: mucosal-to-serosal direction; S-M: serosal-to-mucosal direction. PTX-NP: paclitaxel-loaded poly(anhydride) nanoparticles; PTX-NP2: paclitaxel loaded in nanoparticles pegylated with PEG 2000; PTX-NP6: paclitaxel loaded in nanoparticles pegylated with PEG 6000; PTX-NP10: paclitaxel loaded in nanoparticles pegylated with PEG 10000.

	Experimental conditions	$P_{app}$ ( $10^{-6}$ cm/s)	Absorption enhancement ratio (R)
Taxol <sup>®</sup>	M-S; 37°C	1.2 $\pm$ 0.2	1
PTX-NP	M-S; 37°C	2.1 $\pm$ 0.2	1.8
PTX-NP2	M-S; 37°C	8.5 $\pm$ 0.5***	7.2
PTX-NP2	M-S; 4°C	10 $\pm$ 3***	8.5
PTX-NP2	M-S; Pg – P inhibition (verapamil), 37°C	25 $\pm$ 5***	21
PTX-NP2	M-S; No bioadhesion, 37°C	0.3 $\pm$ 0.5	0.3
PTX-NP6	M-S; 37°C	8.7 $\pm$ 1.5***	7.3
PTX-NP10	M-S; 37°C	4.0 $\pm$ 1.2***	3.3
Taxol <sup>®</sup>	S-M; 37°C	32 $\pm$ 2	27
PTX-NP2	S-M; 37°C	22 $\pm$ 2	18

\*\*\*  $p < 0.005$  all groups vs. commercial Taxol<sup>®</sup> (U Mann-Whitney test).

**Table 3.** Pharmacokinetic parameters of the different formulations tested. PTX-NP: paclitaxel-loaded poly(anhydride) nanoparticles; PTX-NP2: paclitaxel loaded in nanoparticles pegylated with PEG 2000; PTX-NP6: paclitaxel loaded in nanoparticles pegylated with PEG 6000; PTX-NP10: paclitaxel loaded in nanoparticles pegylated with PEG 10000.

Formulation	Route	AUC ( $\mu\text{g h/ml}$ )	$C_{\text{max}}$ ( $\mu\text{g}$ )	$T_{\text{max}}$ (h)	MRT (h)	$T_{1/2z}$ ( $\text{h}^{-1}$ )	$F_r$
Taxol <sup>®</sup>	i.v.	81 $\pm$ 4	204 $\pm$ 2	0.01	1.7 $\pm$ 0.2	2.6 $\pm$ 0.4	100
Taxol <sup>®</sup>	Oral	ND	15	ND	ND	ND	0
PTX-NP2	Oral	56 $\pm$ 3*‡	2.1 $\pm$ 0.1	5.8	26 $\pm$ 1	9.3 $\pm$ 0.5	70
PTX-NP6	Oral	32 $\pm$ 2**†	1.9 $\pm$ 0.1	3.0	27 $\pm$ 1	6.2 $\pm$ 0.3	40
PTX-NP10	Oral	13 $\pm$ 1**	1.4 $\pm$ 0.1	3.3	18 $\pm$ 1	29 $\pm$ 2	16
PTX-NP	Oral	7.4 $\pm$ 0.9**	0.2 $\pm$ 0.0	3.8	31 $\pm$ 1	27 $\pm$ 1	9.1

\* Man-Whitney U-test between PTX-NP2 vs Taxol<sup>®</sup> i.v. ( $p$ -value < 0.05).

\*\* Man-Whitney U-test between PTX-NP6, PTX-NP10 and PTX-NP vs Taxol<sup>®</sup> i.v. ( $p$ -value < 0.01).

† Man-Whitney U-test between PTX-NP6 vs PTX-NP10 and PTX-NP ( $p$ -value < 0.05).

‡ Man-Whitney U-test between PTX-NP2 vs PTX-NP6, PTX-NP10 and PTX-NP ( $p$ -value < 0.01).

AUC<sub>0-∞</sub>: area under the concentration-time curve from time 0 to ∞;  $C_{\text{max}}$ : peak of maximum concentration;  $T_{\text{max}}$ : time to peak concentration; MRT: mean residence time;  $t_{1/2z}$ : half-life of the terminal phase.

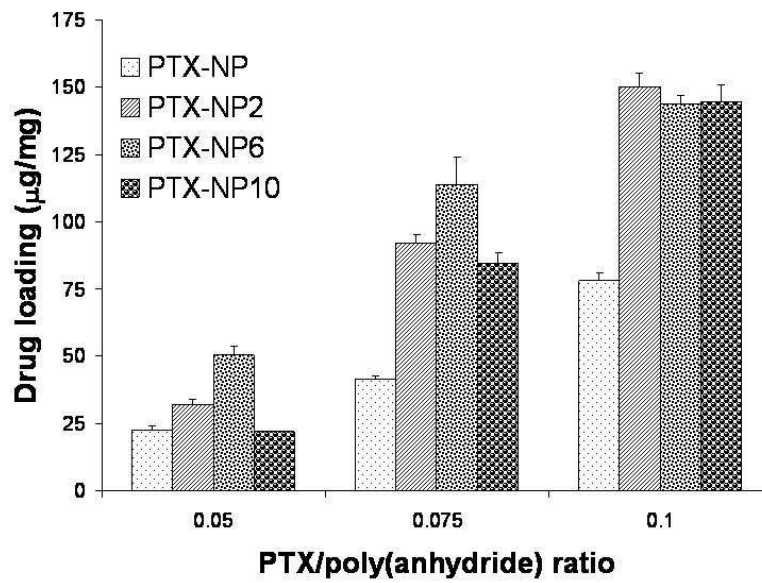


Figure 1. Influence of the PTX/poly(anhydride) ratio on the drug loading of the resulting nanoparticles. Data expressed as the mean±S.D. (n = 3). Experimental conditions: PVM/MA: 100 mg. PEG/poly(anhydride) ratio of 0.125. Incubation time: 1 hour. PTX-NP: paclitaxel-loaded poly(anhydride) nanoparticles; PTX-NP2: paclitaxel loaded in nanoparticles pegylated with PEG 2000; PTX-NP6: paclitaxel loaded in nanoparticles pegylated with PEG 6000; PTX-NP10: paclitaxel loaded in nanoparticles pegylated with PEG 10000.

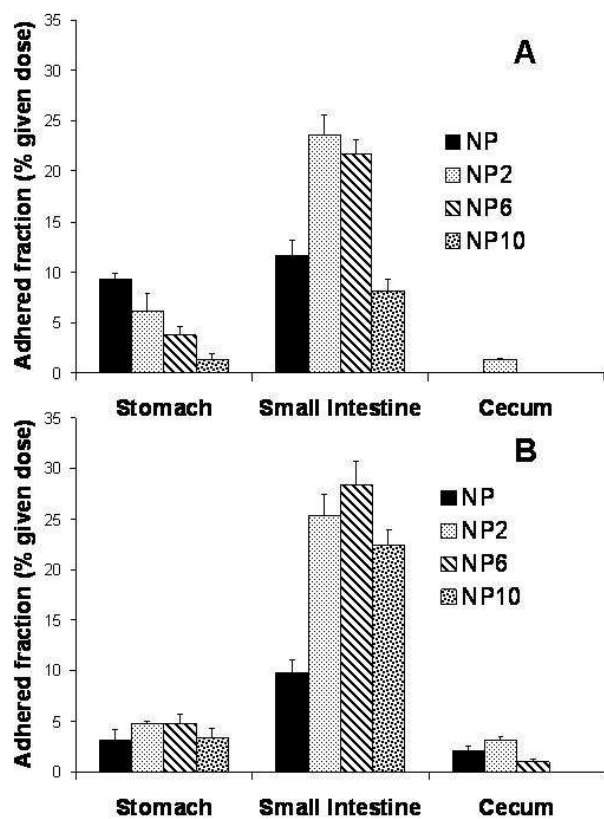


Figure 2. Adhered fractions of nanoparticles in the different parts of rat gastrointestinal tract 1 h (A) and 3 h (B) post-administration. The adhered fractions are presented as a percentage of the initial administered dose (mean  $\pm$  SD; n=6).



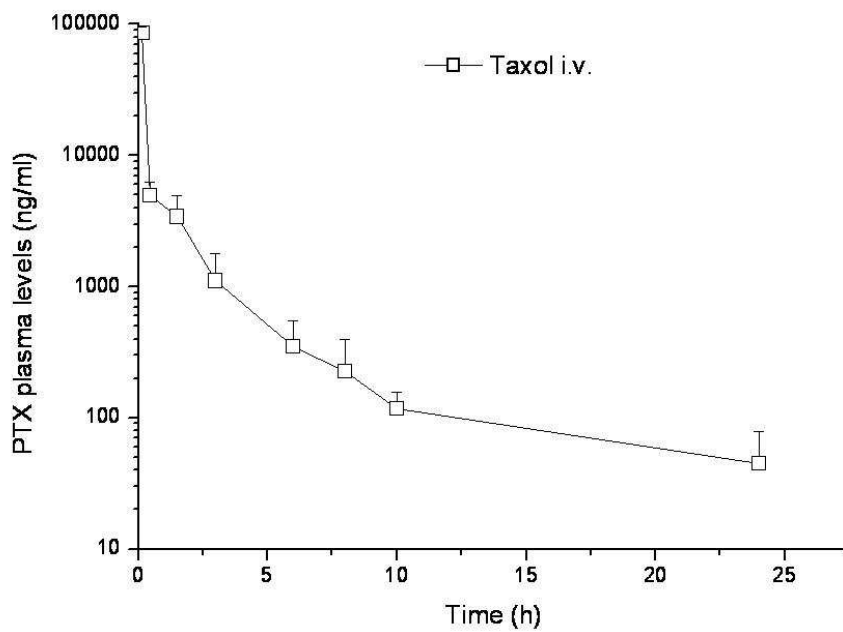


Figure 3. Plasma paclitaxel concentration-time profile after the intravenous administration of a 10 mg/kg dose of Taxol®. Data are expressed as mean  $\pm$  SD, n=6 per time point.

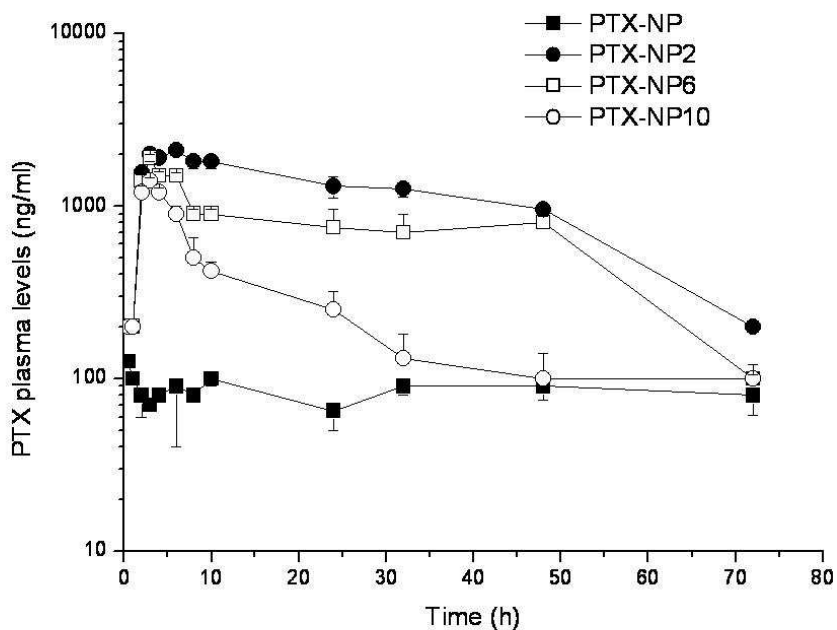


Figure 4. Paclitaxel plasma levels after the oral administration of a single dose of 10 mg/kg. PTX-NP: paclitaxel-loaded poly(anhydride) nanoparticles; PTX-NP2: paclitaxel loaded in nanoparticles pegylated with PEG 2000; PTX-NP6: paclitaxel loaded in nanoparticles pegylated with PEG 6000; PTX-NP10: paclitaxel loaded in nanoparticles pegylated with PEG 10000. Data expressed as mean  $\pm$  SD (n=6).

